Progress In Electromagnetics Research C, Vol. 2, 65–94, 2008

ANALYSIS OF CFAR DETECTION OF FLUCTUATING TARGETS

M. B. El Mashade

Electrical Engineering Department
Faculty of Engineering
Al Azhar University
Nasr City, Cairo, Egypt

Abstract—Our scope in this paper is to provide a complete analysis of CFAR detection of fluctuating targets when the radar receiver incoherently integrates M returned pulses from a chi-squared fluctuating targets with two and four degrees of freedom and operates in a multitarget environment. Since the Swerling models of fluctuating targets represent a large number of such type of radar targets, we restrict our attention here to this interesting class of fluctuation models. There are four categories of such representation; namely SWI, SWII, SWIII, and SWIV. SWI and SWIII represent scan-to-scan fluctuating targets, while SWII and SWIV represent fast pulse-to-pulse fluctuation. Exact expressions are derived for the probability of detection of all of these models. A simple and an effective procedure for calculating the detection performance of both fixed-threshold and adaptive-threshold algorithms is obtained. The backbone of this procedure is the ω-domain representation of the cumulative distribution function of the test statistic of the processor under consideration. In the CFAR case, the estimation of the noise power levels from the leading and the trailing reference windows is based on the OS technique. The performance of this detector is analyzed in the case where the operating environment is ideal and where it includes some of extraneous targets along with the target under test. The primary and the secondary outlying targets are assumed to be fluctuating in accordance with the four Swerling's models cited above. The numerical results show that, for large SNR, the processor detection performance is highest in the case of SWIV model while it attains its minimum level of detection in the case of SWI model. Moreover, SWII model has higher performance than the SWIII representation of fluctuating targets. For low SNR, on the other hand, the reverse of this behavior is occurred. This observation is common either for fixed-threshold or for adaptive-threshold algorithm.

1. INTRODUCTION

Target radar characteristics are the deriving force in the design and performance analysis of all radar systems. The fluctuation rate of a radar target may vary from essentially independent return amplitudes from pulse-to-pulse to significant variation only on a scan-to-scan basis. The Swerling models together with the non-fluctuating bracket the behavior of fluctuating targets of practical interest.

Radar is basically a means of gathering information about distant objects, or targets, by sending electromagnetic waves at them and analyzing the echoes. There are two aspects to the radar statistical problem. The first is concerned with the background noise, which is random in character. In the absence of this background noise, detection poses no difficulty which means that however small the reflected signal from a target, it may be detected with sufficient gain in the receiver. Background noise interference, however, imposes a limit on the minimum detectable signal. The question of target existence is, in fact, a choice of deciding between noise alone or signal-plus-noise. Random noise interference arises from many sources including radiation from the external environment and internal thermal noise. Generally, this noise is wideband with a white or nearly flat spectral density. In addition, there is another major background noise source, which is referred to as a clutter. This type of noise represents the aggregate radar return from a collection of many small scatterers, e.g., ground return, sea return, reflection from rain, chaff, and decay clouds. Detection and estimation in a clutter environment is a major problem in modern radar [1–5].

The second statistical aspect of the radar problem stems from a reflective properties of radar targets. If the radar cross section of an aircraft, or other complex target structures, is observed as a function of aspect angle, the resulting pattern is characterized by rapid fluctuations in amplitude with minute changes in aspect angle. In a typical radar situation, the target is observed many times. The aspect angle at a particular time will govern its observed radar cross section. Since many targets have relative motion with respect to the radar, aspect angle changes on successive observations alter the radio frequency phase relationships, thereby modifying the radar cross section. This change may be a slow variation and occur on a scan-to-scan basis (on successive antenna scans across a target) or it may be on a pulse-to-pulse basis (on successive sweeps). Because the exact nature of the change is difficult to predict, a statistical description is often adopted to characterize the target radar cross section [1, 6–8].

Three families of radar cross section fluctuation models have been

used to characterize most target populations of interest; namely chi-square family, Rice family, and the log-normal family. The χ^2 models are used to represent complex targets, such as aircraft, and have the characteristics that the distribution is more concentrated about the mean as the value of its defined parameter is increased. As special cases of these models, Swerling's versions are derived. This Swerling representation of fluctuating targets brackets the majority of the actual radar targets. In SWI case, the echo pulses received from a target on any one scan are of constant amplitude throughout the entire scan, but are independent (uncorrelated) from scan to scan. A target echo fluctuation of this type is called scan-to-scan fluctuation. It is also known as slow fluctuations. SWII case has the same behavior as SWI except that the fluctuations are independent from pulse to pulse rather than from scan to scan. It is sometimes called fast fluctuations. As in case SWI, the radar cross section is assumed to be constant within a scan and independent from scan to scan; but with a probability density function different to that representing SWI. This probability density function is representative of targets that can be modeled as one scatterer together with a number of small scatterers. Finally, SWIV is characterized by fluctuation from pulse to pulse with the same probability density function as in SWIII [1, 4–6].

The major form of CFAR has been the CA technique. It uses the maximum likelihood estimate of the noise power to set the adaptive threshold. Although the presence of interferers inside the reference window leads to an overestimate of the actual noise power and this in turn gives rise to a masking of legitimate targets, it is still of major importance because it is the optimum CFAR processor when the background noise is homogeneous and the reference cells contain independently, identically, and exponentially distributed observations [7, 9–16].

Analysis of adaptive threshold setting algorithms has generally relied on either Monte-Carlo simulation, or closed form techniques. Monte-Carlo simulation has the drawbacks of both requiring substantial computer time, and lacking precision. Closed-form analysis, when mathematically tractable, is preferable because it yields more precise results in much less computation time. Our object in this paper is to obtain closed-form analysis for fixed threshold as well as CA adaptive threshold schemes when they are used to detect χ^2 models of fluctuating targets, especially, the four different types of Swerling (SWI, SWII, SWIII, and SWIV).

The organization of this paper is as follows: Section 2 describes the system model, formulates the problem under consideration. and computes the characteristic function of the postdetection integrator

output for the case where the signal fluctuation obeys χ^2 statistics. In Section 3, the performance of the processors under consideration is analyzed in nonhomogeneous background environment. Section 4 deals with the numerical results, while Section 5 contains a brief discussion along with our conclusions.

2. GENERAL STATISTICAL MODEL

Detection of signals is equivalent to deciding whether the receiver output is due to noise alone or to signal-plus-noise. This is the type of decision made by a human operator from the information presented on a radar display. When the detection process is carried out automatically by electronic means without the aid of an operator, the detection criterion must be carefully specified and built into the decision made device. The radar detection process was described in terms of threshold detection. The level of this threshold divides the output into a region of no detection (H_0) and a region of detection (H_1). By raising or lowering this bias level, the number of times a noise pulse surpasses the bias level either decreases or increases, respectively. The setting of this level depends on the number of times that noise will be permitted to exceed the bias level during a given period of time. To mistake a noise pulse for a signal return is called a false alarm. To mistake a signal return for a noise pulse is called miss detection. Miss detection and false alarm, therefore, are subject to tradeoff.

An adaptive threshold detector is an algorithm which provides a constant false alarm rate in a varying nonhomogeneous clutter and noise interference environment by adaptively adjusting the detection threshold. This procedure assumes that the general form of the interference's probability distribution is known except for a small number of unknown parameters. These unknown parameters are estimated on a cell-to-cell basis by examining reference cells surrounding the cell under test. The resulting estimated interference probability distribution function is then used in each cell to obtain a threshold setting that provides the desired probability of false alarm. Fig. 1 is a useful way of depicting the CFAR detection technique of a radar target in the case of noncoherent integration of M-pulses.

Under certain conditions, usually met in practice, maximizing the output peak signal-to-noise ratio (SNR) of a radar receiver maximizes the detectability of a target. A linear network that does this is called a matched filter. Thus, a matched filter is the basis for the design of almost all radar receiver. The square-law device demodulates the baseband signal and M consecutive sweeps are incoherently integrated to represent the input of the adaptive technique. The box labeled

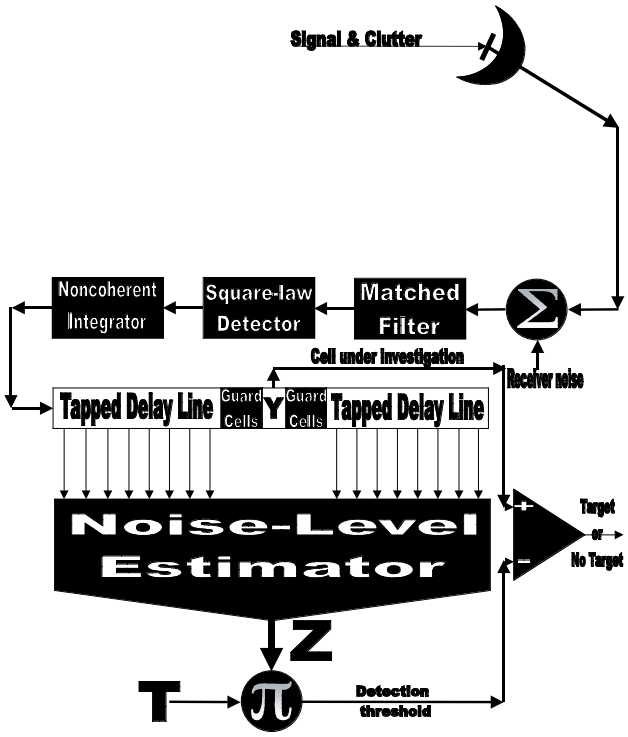

Figure 1. Block diagram of CFAR detection of radar target.

cell under test represents the radar range cell that is currently being examined for the presence of a target. Buffer cells adjacent to the cell under test can be used to avoid contamination with the edge of the matched filter output from the target return. Two tapped delay lines sample echo signals in a number of reference cells located on both sides of the range cell of interest. The spacing between reference cells is equal to the radar range resolution which is usually equal to the pulse width. The statistic Z which is proportional to the estimate of total noise power is constructed by processing the contents of N reference cells surrounding the cell under investigation whose content is denoted by ν. A target is declared to be detected if ν exceeds the threshold ZT, where T is a constant scale factor used to achieve the required rate of false alarm for a given window size when the background noise is homogeneous. The processor configuration varies with different CFAR algorithms.

Our approach in analyzing a CFAR processor is to evaluate its

probability of detection which is defined as

$$P_d \triangleq Pr\{\nu \rangle TZ|H_1\} \tag{1}$$

This definition can be formulated in another simpler form as

$$P_d \triangleq Pr\{Z \langle \nu/T|H_1\} \tag{2}$$

In term of the probability density functions (PDF's) of ν and Z, Eq. (2) can be formulated as

$$P_d = \int_0^\infty f_\nu(\nu) \int_0^{\nu/T} f_z(x)dxd\nu \tag{3}$$

It is important to note that the inner integration in the above expression represents the cumulative distribution function (CDF) of the random variable (RV) Z. Thus,

$$P_d = \int_0^\infty f_\nu(\nu)F_z(\nu/T)d\nu \tag{4}$$

Another important version of Eq. (4) has an expression given by

$$P_d = T\int_0^\infty f_\nu(T\nu)F_z(\nu)d\nu \tag{5}$$

From the definition of Laplace transformation, P_d can be put in a more simpler form as

$$P_d = TG_t(\omega)\Big|_{\omega=0} \tag{6}$$

where $G_t(\omega)$ denotes the Laplace transformation of the integrand of Eq. (5).

$$\begin{aligned} G_t(\omega) &\triangleq \int_0^\infty f_\nu(T\nu)F_z(\nu)\exp(-\omega\nu)d\nu \\ &= \frac{1}{T}\Phi_\nu(\omega/T) * \Psi_z(\omega) \end{aligned} \tag{7}$$

In the previous expression, the * symbol represents the mathematical convolution, $\Phi_\nu(.)$ denotes the characteristic function (CF) of the RV ν, and $\Psi(.)$ represents the Laplace transformation of the CDF of the

RV Z. Finally, the detection probability takes the following analytical form

$$P_d = \frac{1}{2\pi j} \oint_{C^-} \Phi_\nu(u/T)\Psi_z(\omega - u)du\Big|_{\omega=0} \tag{8}$$

The contour of integration C^- consists of a vertical path in the complex u-plane crossing the negative real axis at the rightmost negative real axis singularity of $\Phi_\nu(.)$ and closed in an infinite semicircle in the left half plane.

From Eq. (8), it is evident that the CF of the RV that represents the content of the cell under test plays an important role in determining the processor detection performance. Let us now calculate this very interesting function for the four cases of Swerling representation of fluctuating targets.

In the analysis that follows, it is assumed that the clutter background is homogeneous over the area encompassed by the delay line. This means that the PDF of the output from any delay line tap with no target return present is

$$f_\nu(x) = \frac{1}{\psi} e^{-x/\psi} U(x) \tag{9}$$

The unknown average noise power is denoted by ψ in the above formula and the unit-step function is denoted by $U(.)$. The delay line outputs are assumed to be statistically independent RV's. When a nonfluctuating target return-plus-noise is present in any tap, on the other hand, the output of this tap has a PDF given by [5]

$$f_\nu(x) = \frac{1}{\psi} I_0\left(2\frac{\sqrt{xA}}{\psi}\right) \exp\left(-\frac{x+A}{\psi}\right) U(x) \tag{10}$$

A/ψ denotes the signal-to-noise ratio (SNR) at the square-law detector input and $I_0(.)$ represents the modified Bessel function of type 1 and of order 0. When the target return present in one of the tap outputs comprising the sum of M-pulses, which are noncoherently integrated, i.e.,

$$Q \triangleq \sum_{\ell=1}^{M} \nu_\ell \tag{11}$$

has a PDF of the form [12]

$$f_Q(x) = \frac{1}{\psi}\left(\frac{x}{A}\right)^{\frac{M-1}{2}} I_{M-1}\left(2\frac{\sqrt{xA}}{\psi}\right) \exp\left(-\frac{x+A}{\psi}\right) U(x) \tag{12}$$

The CF associated with this PDF can be easily calculated and the result can be put as

$$\Phi_Q(\omega/A) = \left(\frac{1}{\psi\omega + 1}\right)^M \exp\left(-\frac{\omega A}{\psi\omega + 1}\right) \tag{13}$$

The unconditional CF is now obtained by averaging the previous expression over the target fluctuation distribution of A. For chi-square family of target models, the RV A has a PDF given by [4]

$$f_A(A\sqrt{A}) = \frac{1}{\Gamma(K)}\left(\frac{K}{\overline{A}}\right)^K A^{K-1}\exp\left(-K\frac{A}{\overline{A}}\right)U(A) \tag{14}$$

$\overline{A}$ denotes the average M-pulse SNR and $K > 0$ represents a fluctuation parameter. The unconditional CF is then calculated as

$$\begin{aligned}\Phi_Q(\omega/A) &\triangleq \int_0^\infty \Phi_Q(\omega/A) f_A(A\sqrt{A})dA \\ &= \left(\frac{1}{\psi\omega+1}\right)^{M-K}\left(\frac{1}{\beta\omega+1}\right)^K,\ \beta \triangleq \psi\left(1+\frac{\overline{A}/\psi}{K}\right)\end{aligned} \tag{15}$$

Eq. (15) is the fundamental expression from which the Swerling models are derived as special cases as we shall see in the next section.

3. CALCULATION OF PROBABILITY OF DETECTION OF FLUCTUATING TARGETS

Now, we are going to evaluate the detection performance of the adaptive threshold setting techniques for the fluctuating targets of Swerling models.

1- Swerling I case (SWI):

In this case, the fluctuation parameter K has a unit value. Letting $K = 1$ in Eq. (15) yields

$$\Phi_Q(\omega) = \left(\frac{1/\psi}{\omega + 1/\psi}\right)^{M-1}\left(\frac{1/\alpha}{\omega+1/\alpha}\right),\ \alpha \triangleq \psi(1+\overline{A}/\psi) = \psi(1+M\overline{A}_1) \tag{16}$$

In the above expression, $\overline{A}_1$ represents the average per pulse SNR. The substitution of this expression into Eq. (8) gives

$$P_d = \frac{T}{\alpha}\left(\frac{1/\psi}{1/\psi - 1/\alpha}\right)^{M-1}\Psi_z(T/\alpha) + \frac{(T/\psi)^{M-1}}{\alpha} + \left(\frac{T}{\psi}\right)^{M-1}\left(\frac{T}{\alpha}\right)$$

$$\times \frac{1}{\Gamma(M-1)} \frac{d^{M-2}}{du^{M-2}} \left\{ \left(\frac{1}{u+T/\alpha} \right) \Psi_z(-u) \right\} \Bigg|_{u=-T/\psi} \tag{17}$$

2- Swerling II case (SWII):

This fluctuation model is characterized by $K = M$, the substitution of which into Eq. (15) gives

$$\Phi_Q(\omega) = \left(\frac{1/\alpha}{\omega + 1/\alpha} \right)^M, \quad \alpha \triangleq \psi \left(1 + \frac{\overline{A}/\psi}{M} \right) = \psi(1 + \overline{A}_1) \tag{18}$$

In this case, the processor detection performance takes the form

$$P_d = \left(\frac{T}{\alpha} \right)^M \frac{(-1)^{M-1}}{\Gamma(M)} \frac{d^{M-1}}{du^{M-1}} \{ \Psi_z(u) \} \Big|_{u=T/\alpha} \tag{19}$$

3- Swerling III case (SWIII):

By letting $K = 2$ in the general expression of Eq. (15), the resulting model is known as SWIII which has a CF of the form

$$\begin{aligned} \Phi_Q(\omega) &= \left(\frac{1/\psi}{\omega + 1/\psi} \right)^{M-2} \left(\frac{1/\alpha}{\omega + 1/\alpha} \right)^2 \\ \alpha &\triangleq \psi \left(1 + \frac{\overline{A}/\psi}{M} \right) = \psi \left(1 + M \frac{\overline{A}_1}{2} \right) \end{aligned} \tag{20}$$

The probability of detecting a fluctuating target of SWIII model becomes

$$\begin{aligned} P_d = \left(\frac{T}{\alpha} \right)^2 \left(\frac{T}{\psi} \right)^{M-2} \Bigg\{ & \frac{d}{du} \left[\left(\frac{1}{u+T/\psi} \right)^{M-2} \Psi_z(-u) \right] \Bigg|_{u=-T/\alpha} \\ & + \frac{1}{\Gamma(M-2)} \frac{d^{M-3}}{du^{M-3}} \left[\left(\frac{1}{u+T/\alpha} \right)^2 \Psi_z(-u) \right] \Bigg|_{u=-T/\psi} \Bigg\} \end{aligned} \tag{21}$$

4- Swerling IV case (SWIV):

The characterization of this fluctuation model is $K = 2M$. Thus, the substitution of this value into Eq. (15) yields

$$\begin{aligned} \Phi_Q(\omega) &= \left(\frac{1/\psi}{\omega + 1/\psi} \right)^{-M} \left(\frac{1/\alpha}{\omega + 1/\alpha} \right)^{2M} \\ \alpha &\triangleq \psi \left(1 + \frac{\overline{A}/\psi}{2M} \right) = \psi \left(1 + \frac{\overline{A}_1}{2} \right) \end{aligned} \tag{22}$$

The detection performance of the adaptive processor for this type of fluctuating targets is

$$P_d = \left(\frac{T}{\alpha}\right)^{2M}\left(\frac{T}{\psi}\right)^{-M}\frac{1}{\Gamma(2M)}\frac{d^{2M-1}}{du^{2M-1}}\left\{\left(\frac{1}{u+T/\psi}\right)^{-M}\Psi_z(-u)\right\}\Bigg|_{u=-T/\alpha} \tag{23}$$

In the absence of the radar target ($\alpha = \psi$), the CF of the cell under test which represents the no target hypothesis (null hypothesis) takes a very simplified expression of the form

$$\Phi_Q(\omega) = \left(\frac{1}{\psi\omega + 1}\right)^M \triangleq \Phi_c(\omega) \tag{24}$$

The detection probability in this case tends to the probability of false alarm which becomes

$$P_{fa} = \left(\frac{T}{\psi}\right)^M \frac{1}{\Gamma(M)}\frac{d^{M-1}}{du^{M-1}}\left\{\Psi_{Z_f}(-u)\right\}\Big|_{u=-T/\psi} \tag{25}$$

Eqs. (17), (19), (21), (23), (25) are the basic analytical formulas of our analysis in this manuscript. These expressions are general for any CFAR detector. Our scope in the remaining part is to evaluate the performance of the fixed-threshold as well as one of the most important adaptive-threshold (CA) detectors to determine their behavior against fluctuating targets of Swerling models. By examining the above formulas, it is obvious that they rely on the Laplace transformation of the CDF of the noise power level estimate Z and its mathematical differentiation. Therefore, we are interested in formulating this transformation when the detection scheme operates in an environment that contains several extraneous targets along with the target under investigation.

4. PROCESSOR DETECTION PERFORMANCE

Here, we are interested in applying the previously derived formulas to the optimum detector, against which any proposed processor is compared, and one of the most popular and efficient scheme in maintaining a constant rate of false alarm against environmental impairments which is known as ordered-statistics (OS) detector. We are going to evaluate their performance against fluctuating targets of Swerling models.

4.1. Fixed-Threshold Detector

The useful procedure for establishing the decision threshold at the output of the radar receiver is based on the classical statistical theory of the Neyman-Pearson criterion which is described in terms of the two types of errors that might be made in the detection decision process. One type of these errors is to mistake noise for signal when only noise is present. It occurs whenever the noise out of the receiver is large enough to exceed the decision threshold level. In statistics, this is called a false alarm. The other type of these errors occurs when a signal is present but is erroneously considered to be noise. The radar engineer would call such an error a missed detection. It might be desired to minimize both errors, but they both cannot be minimized independently. In the Neyman-Pearson theory, the probability of first type error is fixed and the probability of the second type error is minimized. Since the threshold level is set in such a way that a specified probability of false alarm is not exceeded, this is equivalent to fixing the probability of type one error and minimizing the type two error (or maximizing the detection probability. This is the Neyman-Pearson test used in statistics for determining the validity of a specified statistical hypothesis. It is employed in most radars for making the detection decision.

The optimum detector sets a fixed threshold to determine the presence of a target under the assumption that the total homogeneous noise power "ψ" is known a priori. In this case, the detection probability is given by

$$\begin{aligned} P_d &\triangleq Pr\{Q \rangle Q_0 | H_1\} = \int_{Q_0}^{\infty} f_Q(y)dy \\ &= \int_0^{\infty} f_Q(y)dy - \int_0^{Q_0} f_Q(y)dy = 1 - F_Q(Q_0) \end{aligned} \tag{26}$$

From the above expression, it is obvious that the CDF of the content of the cell under test is the backbone of the analysis of the fixed-threshold detector, Once the CF of Q is calculated, the Laplace transformation of its CDF is consequently obtained as [7]

$$\Psi_Q(\omega) = \frac{\Phi_Q(\omega)}{\omega} \tag{27}$$

Once the ω-domain representation of CDF of Q is computed, its t-domain representation can be easily obtained through the Laplace

inverse technique. For simplicity, we will consider in the following $\psi = 0$. Thus,

$$F_{SWI}(z) = 1 - \frac{1}{(1-b)^{M-1}} \exp(-bz) + \sum_{j=0}^{M-2} \frac{\eta_j}{\Gamma(M-j-1)} z^{M-j-2} \exp(-z) \tag{28}$$

with

$$b \triangleq \frac{1}{1+MA} \quad \text{and} \quad \eta_j \triangleq \left(\frac{1}{1-b}\right)^{j+1} - 1 \tag{29}$$

$$F_{SWII}(z) = 1 - \sum_{\ell=0}^{M-1} \frac{\alpha^{M-\ell-1}}{\Gamma(M-\ell)} z^{M-\ell-1} \exp(-a\ z) \text{ with } \alpha \triangleq \frac{1}{1+A} \tag{30}$$

$$\begin{aligned} F_{SWIII}(z) \ &= \ 1 + \sum_{\ell=0}^{1} \frac{\beta_\ell}{\Gamma(2-\ell)} z^{2-\ell-1} \exp(-cz) \\ &\quad + \sum_{\lambda=0}^{M-3} \frac{\zeta_\lambda}{\Gamma(M-\lambda-2)} z^{M-\lambda-3} \exp(-z) \end{aligned} \tag{31}$$

with

$$c \ \triangleq \ \left(1 + M\frac{A}{2}\right)^{-1} \tag{32a}$$

$$\zeta_\lambda \ \triangleq \ \left(\frac{1}{1-c}\right)^{\lambda+1} - c\frac{(2)_\lambda}{(1-c)^\lambda} - 1 \tag{32b}$$

$$\beta_\ell \ \triangleq \ -c^{1-\ell} - (-1)^\ell c^2 \sum_{k=0}^{M-3} \frac{(M-k-2)}{(1-c)^{M+\ell-k-2}} \tag{32c}$$

The Pochhammer symbol $(x)_j$ is defined as:

$$(x)_j \triangleq \begin{cases} 1 & \text{for} \quad j = 0 \\ x(x+1)(x+2)\ldots(x+j-1) & \text{for} \quad j > 0 \end{cases} \tag{33}$$

and

$$\begin{aligned} F_{SWIV}(z) \ &= \ \sum_{\ell=0}^{M} \binom{M}{\ell} (1-\xi)^\ell \\ &\quad \times \left\{ \xi^{M-\ell} - \sum_{\lambda=0}^{M+\ell-1} \frac{\xi^{2M-\lambda-1}}{\Gamma(M+\ell-\lambda)} z^{M+\ell-\lambda-1} \exp(-\xi z) \right\} \end{aligned} \tag{34}$$

with

$$\xi \triangleq \left(1 + \frac{A}{2}\right)^{-1} \tag{35}$$

Consequently, the processor performance against SWI, SWII, SWIII, and SWIV target fluctuation models is now completely determined.

4.2. Adaptive-Threshold Detector

Since the clutter plus noise power is not known at any given location, a fixed-threshold detection scheme can not be applied to the radar returns if the rate of false alarm is required to be controlled. Moreover, radar performance is often degraded by the presence of false targets. To reduce this effect, radar detection processing can use an algorithm to estimate the clutter energy in the tested cell and then adjust the constructed threshold to reflect changes in this energy at different test cell positions. An attractive class of schemes that can be used to overcome the problem of clutter is that of CFAR type which set the threshold adaptively based on local information of total noise power. In other words, the CFAR detection is one of the desirable features for radar receivers. Since the OS based algorithm has an immunity to the presence of extraneous targets amongst the contents of reference samples, we are going to evaluate its performance in detecting fluctuating radar targets.

As we have previously shown in Section 3, the detection performance of an adaptive-threshold scheme depends mainly on the calculation of the Laplace transformation of the CDF of its noise power level estimate Z. Hence, all we need in the analysis of this type of detection techniques is the computation of the CF of its background noise level and this is our scope in the rest of this section.

The amplitude values taken from the reference window, of size N, are first rank-ordered according to their increasing magnitude. The sequence thus achieved is

$$q_{(1)} \leq q_{(2)} \leq q_{(3)} \leq \ldots \leq q_{(K)} \leq \ldots \leq q_{(N)} \tag{36}$$

The indices in parentheses indicate the rank-order number. $q_{(1)}$ denotes the minimum and $q_{(N)}$ the maximum value. The sequence given in Eq. (36) is called an ordered-statistic. The central idea of an ordered statistic CFAR processor is to select one certain value from the above sequence and to use it as an estimate Z for the average clutter power as observed in the reference window. Thus,

$$Z_{OS} = q_{(K)}, \qquad K \in \{1, 2, 3, \ldots, N\} \tag{37}$$

Since the nonhomogeneous situation is more general than the homogeneous case, we are going to analyze the performance of OS detector when the operating environment is of multiple-target situation. The multiple target situation is frequently encountered in practice in which the reference window contains nonuniform samples. This may occur in a dense environment where two or more potential targets appear in the range cells surrounding the cell under test. The amplitudes of all the interfering target returns that may be present amongst the candidates of the reference window are assumed to be of the same strength and to fluctuate in accordance with Swerling models. The interference-to-noise ratio (INR) for each of the spurious targets is taken as a common parameter and is denoted by I. Thus, for reference cells containing extraneous target returns, the total background noise power is $\psi(1+I)$, while the remaining reference cells have identical noise power of ψ value. Suppose that the reference set of size N contains r cells from interfering target returns with background power level of $\psi(1+I)$ and the remaining $N-r$ cells from clear background with noise power ψ. Thus, the noise power level of this set is estimated as

$$F_{OS}(z) = \sum_{i=K}^{N} \sum_{j=\max(0,i-r)}^{\min(i,N-r)} \binom{N-r}{j} \binom{r}{i-j} \times [1-F_t(z)]^{N-r-j} \{F_t(z)\}^j [1-F_s(z)]^{r-i+j} \{F_s(z)\}^{i-j} \quad (38)$$

where $F_t(z)$ represents the CDF of the reference cell that contains thermal noise only of power ψ, and $F_s(z)$ denotes the CDF of the reference cell that contains interfering target return. Therefore,

$$F_t(z) = 1 - \sum_{\ell=0}^{M-1} \frac{z^{M-\ell-1}}{\Gamma(M-\ell)} \exp(-z) U(z) \quad (39)$$

On the other hand, the CDF of the reference cell that contains a spurious fluctuating target return was previously calculated for the four Swerling fluctuating models which can be considered as special cases from the general expression's form [14]

$$F_s(z) = L^{-1}\left\{ \frac{1}{\omega} \prod_{\ell=1}^{M} \frac{1}{1+(1+I\lambda_\ell)\omega} \right\} = 1 - \sum_{\ell=1}^{M} \gamma_\ell e^{-c_\ell z} \quad (40)$$

where L^{-1} denotes the Laplace inverse operator and

$$\gamma_\ell \triangleq \prod_{\substack{k=1 \\ k\neq\ell}}^{M} \frac{1+I\lambda_\ell}{I(\lambda_\ell - \lambda_k)} \quad \text{and} \quad c_\ell \triangleq \frac{1}{1+I\lambda_\ell} \quad (41)$$

when this target fluctuates in accordance with χ^2 with two degrees of freedom. On the other hand, if the interfering target's fluctuation follows χ^2 model with four degrees of freedom, $F_s(z)$ takes the form [15]

$$F_s(z) = L^{-1}\left\{\frac{1}{\omega}\prod_{j=1}^{M}\varepsilon_j^2\frac{\omega+1}{(\omega+\varepsilon_j)^2}\right\} = 1-\sum_{j=1}^{M}(a_j+zt_j)\exp(-\varepsilon_j z) \quad (42)$$

with

$$a_j \triangleq \varepsilon_j(1-\varepsilon_j)^M\prod_{\substack{i=1\\ i\neq j}}^{M}\left(\frac{\varepsilon_i}{\varepsilon_i-\varepsilon_j}\right)^2\left\{\frac{M}{1-\varepsilon_j}+\frac{1}{\varepsilon_j}-\prod_{\substack{\ell=1\\ \ell\neq j}}^{M}\frac{2}{\varepsilon_\ell-\varepsilon_j}\right\} \quad (43)$$

and

$$t_j \triangleq \varepsilon_j(1-\varepsilon_j)\prod_{\substack{k=1\\ k\neq j}}^{M}\varepsilon_k^2\frac{1-\varepsilon_j}{(\varepsilon_k-\varepsilon_j)^2} \quad \text{and} \quad \varepsilon_j \triangleq \left(1+I\frac{\lambda_j}{2}\right)^{-1} \quad (44)$$

To calculate the Laplace transformation of Eq. (38), we rewrite it in another simpler form as

$$\begin{aligned} F_{OS}(z) = &\sum_{i=K}^{N}\sum_{j=\max(0,i-r)}^{\min(i,N-r)}\binom{N-r}{j}\binom{r}{i-j}\\ &\times\sum_{k=0}^{j}\sum_{\ell=0}^{i-j}\binom{j}{k}\binom{i-j}{\ell}(-1)^{i-k-\ell}\\ &\times\{1-F_t(z)\}^{N-r-k}\{1-F_s(z)\}^{r-\ell} \end{aligned} \quad (45)$$

The substitution of Eqs. (39) and (40) into Eq. (45) yields

$$\begin{aligned} F_{OS}(z) = &\sum_{i=K}^{N}\sum_{j=\max(0,i-r)}^{\min(i,N-r)}\binom{N-r}{j}\binom{r}{i-j}\\ &\times\sum_{k=0}^{j}\sum_{\ell=0}^{i-j}\binom{j}{k}\binom{i-j}{\ell}(-1)^{i-k-\ell}\\ &\times\left\{\sum_{m=0}^{M-1}\frac{(z)^m}{\Gamma(m+1)}e^{-z}\right\}^{N-r-k} * \left\{\sum_{n=1}^{M}\gamma_n e^{-c_n z}\right\}^{r-\ell} \end{aligned} \quad (46)$$

The Laplace transformation of the above equation gives

$$\begin{aligned}\Psi_{OS}(\omega) = &\sum_{i=K}^{N}\sum_{j=\max(0,i-r)}^{\min(i,N-r)}\binom{N-r}{j}\binom{r}{i-j}\\ &\times\sum_{k=0}^{j}\sum_{\ell=0}^{i-j}\binom{j}{k}\binom{i-j}{\ell}(-1)^{i-k-\ell}\\ &\times\sum_{\theta_0=0}^{N-r-k}\sum_{\theta_1=0}^{N-r-k}\cdots\sum_{\theta_{M-1}=0}^{N-r-k}\frac{\Omega(N-r-k;\theta_0,\ldots,\theta_{M-1})}{\prod_{\nu=0}^{M-1}[\Gamma(\nu+1)]^{\theta_\nu}}\\ &\times\sum_{\vartheta_1=0}^{r-\ell}\sum_{\vartheta_2=0}^{r-\ell}\cdots\sum_{\vartheta_M=0}^{r-\ell}\Omega(r-\ell;\vartheta_1,\ldots,\vartheta_M)\\ &\times\prod_{\xi=1}^{M}(\gamma_\xi)^{\vartheta_\xi}\frac{\Gamma\left(\sum_{\alpha=0}^{M-1}\alpha\theta_\alpha+1\right)}{\left(\omega+N-r-k+\sum_{\zeta=1}^{M}\vartheta_\zeta c_\zeta\right)^{\sum_{\alpha=0}^{M-1}\alpha\theta_\alpha+1}}\end{aligned}\tag{47}$$

By substituting Eqs. (39), (42) into Eq. (45) one obtains, for χ^2 target fluctuation with four degrees of freedom,

$$\begin{aligned}F_{OS}(z) = &\sum_{i=K}^{N}\sum_{j=\max(0,i-r)}^{\min(i,N-r)}\binom{N-r}{j}\binom{r}{i-j}\\ &\times\sum_{k=0}^{j}\sum_{\ell=0}^{i-j}\binom{j}{k}\binom{i-j}{\ell}(-1)^{i-k-\ell}\\ &\times\left\{\sum_{m=0}^{M-1}\frac{z^m}{\Gamma(m+1)}e^{-z}\right\}^{N-r-k}*\left\{\sum_{n=1}^{M}(a_n+zt_n)\exp(-\varepsilon_n z)\right\}^{r-\ell}\end{aligned}\tag{48}$$

By using the binomial theorem, we can expand the bracketed quantities as a binomial of z. In other words, the above formula can be rewritten as

$$F_{OS}(z) = \sum_{i=K}^{N}\sum_{j=\max(0,i-r)}^{\min(i,N-r)}\binom{N-r}{j}\binom{r}{i-j}$$

$$\times \sum_{k=0}^{j} \sum_{\ell=0}^{i-j} \binom{j}{k} \binom{i-j}{\ell} (-1)^{i-k-\ell}$$
$$\times \sum_{\theta_0=0}^{N-r-k} \sum_{\theta_1=0}^{N-r-k} \cdots \sum_{\theta_{M-1}=0}^{N-r-k} \frac{\Omega(N-r-k;\theta_0,\ldots,\theta_{M-1})}{\prod_{\nu=0}^{M-1} [\Gamma(\nu+1)]^{\theta_\nu}}$$
$$\times \sum_{\gamma=0}^{r-\ell} \binom{r-\ell}{\gamma} \sum_{\xi_1=0}^{\gamma} \sum_{\xi_2=0}^{\gamma} \cdots \sum_{\xi_M=0}^{\gamma} \Omega(\gamma,\xi_1,\xi_2,\ldots,\xi_M)$$
$$\times \sum_{\zeta_1=0}^{r-\ell-\gamma} \sum_{\zeta_2=0}^{r-\ell-\gamma} \cdots \sum_{\zeta_M=0}^{r-\ell-\gamma} \Omega(r-\ell-\gamma,\zeta_1,\zeta_2,\ldots,\zeta_M)$$
$$\times \prod_{i=1}^{M} (t_i \zeta_i a_i \xi_i) z^{\left(r-\ell-\gamma+\sum_{\alpha=10}^{M-1} \alpha\theta_\alpha\right)}$$
$$\times \exp\left(-\left(N-r-k+\sum_{\eta=1}^{M}(\xi_\eta+\zeta_\eta)\varepsilon_\eta\right)z\right) \tag{49}$$

To determine the detection performance of the OS-CFAR processor, it is important to calculate the Laplace transform for its test statistic, where the false alarm and detection probabilities are completely dependent on this transformation and its derivatives with respect to ω. This transformation becomes

$$\Psi_{OS}(\omega) = \sum_{i=K}^{N} \sum_{j=\max(0,i-r)}^{\min(i,N-r)} \binom{N-r}{j} \binom{r}{i-j}$$
$$\times \sum_{k=0}^{j} \sum_{\ell=0}^{i-j} \binom{j}{k} \binom{i-j}{\ell} (-1)^{i-k-\ell}$$
$$\times \sum_{\theta_0=0}^{N-r-k} \sum_{\theta_1=0}^{N-r-k} \cdots \sum_{\theta_{M-1}=0}^{N-r-k} \frac{\Omega(N-r-k;\theta_0,\ldots,\theta_{M-1})}{\prod_{\nu=0}^{M-1} [\Gamma(\nu+1)]^{\theta_\nu}}$$
$$\times \sum_{\gamma=0}^{r-\ell} \binom{r-\ell}{\gamma} \sum_{\xi_1=0}^{\gamma} \sum_{\xi_2=0}^{\gamma} \cdots \sum_{\xi_M=0}^{\gamma} \Omega(\gamma,\xi_1,\xi_2,\ldots,\xi_M)$$
$$\times \sum_{\zeta_1=0}^{r-\ell-\gamma} \sum_{\zeta_2=0}^{r-\ell-\gamma} \cdots \sum_{\zeta_M=0}^{r-\ell-\gamma} \Omega(r-\ell-\gamma,\zeta_1,\zeta_2,\ldots,\zeta_M)$$

$$\times \prod_{i=1}^{M}(t_i\zeta_i a_i\xi_i)\frac{\Gamma\left(r-\ell-\gamma+\sum\limits_{\alpha=10}^{M-1}\alpha\theta_\alpha+1\right)}{\left(\omega+N-r-k+\sum\limits_{\eta=1}^{M}(\xi_\eta+\zeta_\eta)\varepsilon_\eta\right)^{\left(r-\ell-\gamma+\sum\limits_{\alpha=10}^{M-1}\alpha\theta_\alpha+1\right)}} \tag{50}$$

where the definition of the term $\Omega(L; j_1, j_2, \ldots, j_M)$ is as indicated in [13]

$$\Omega(L; i_1, i_2, \ldots, i_M) \triangleq \begin{cases} \dfrac{\Gamma(L+1)}{\prod\limits_{\ell=1}^{M}\Gamma(j_\ell+1)} & \text{for} \quad L=\sum\limits_{\ell=1}^{M} j_\ell \\ 0 & \text{for} \quad L\neq\sum\limits_{\ell=1}^{M} j_\ell \end{cases} \tag{51}$$

Again, the OS-CFAR processor performance is highly dependent upon the value of K. For example, if a single extraneous target appears in the reference window of appreciable magnitude, it occupies the highest ranked cell with high probability. If K is chosen to be N, the estimate will almost always set the threshold based on the value of interfering target. This increases the overall threshold and may lead to a target miss. If, on the other hand, K is chosen to be less than the maximum value, the OS-CFAR scheme will be influenced only slightly for up to N-K spurious targets.

5. PROCESSOR PERFORMANCE ASSESSMENT

We are interested here with the numerical results of the analytical expressions that we are previously derived to take an idea about the behavior of the selected CFAR detector, along with the well-known optimum detector, in detecting χ^2 fluctuating targets when the operating environment is ideal; free of any impurities; as well as in the case where the reference channels are contaminated with returns from extraneous targets. The detection analytical formulas are programmed on a PC digital system for some parameter values and the results of these programs are presented in several categories of curves. The reference window size is chosen to have 24 samples, the ordered-statistic parameter is taken as 21; which is the optimum value for the selected window size, and the design false alarm rate is suggested to be 10^{-6}.

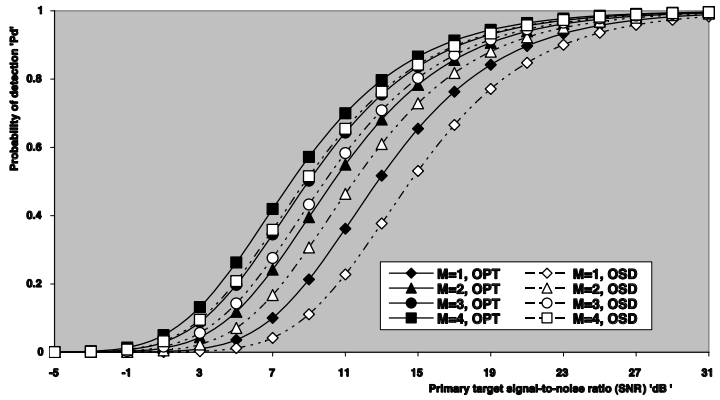

Figure 2. M-sweeps detection performance of OS(21) along with fixed threshold detectors for fluctuating targets of SWI model when $N = 24$, and $P_{fa} = 1.0\text{E-}6$.

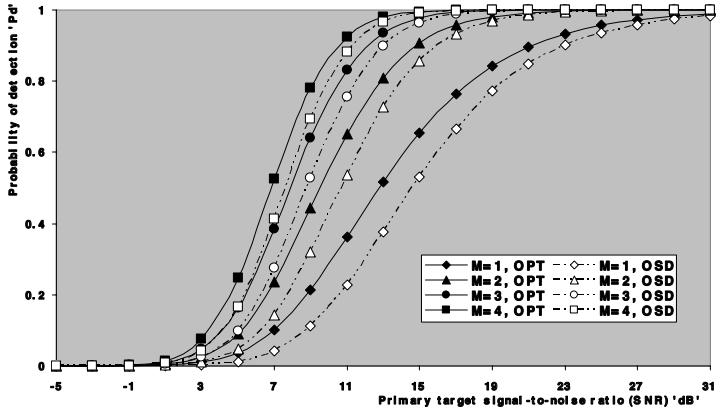

Figure 3. M-sweeps detecti on performance of OS(21) al ong with fi xed threshold detectors for fluctuati ng targets of SWII model when $N = 24$, and $P_{fa} = 1.0\text{E-}6$.

The first category, Figs. 2–5, depicts the detection performance of the CFAR detector, OS(21), when the primary target fluctuates following SWI, SWII, SWIII, and SWIV, respectively. in the case where radar receiver video integrates M-consecutive sweeps. The results of the fixed-threshold detector for the same parameter values and for the same type of target fluctuation are also incorporated in the corresponding figures for the comparison to be an easy task. Moreover, the monopulse

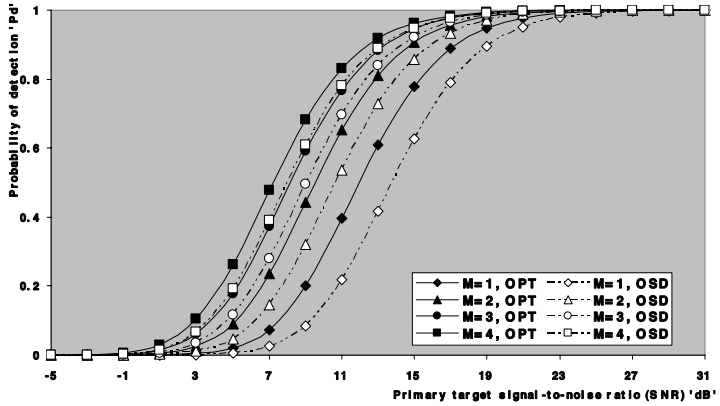

Figure 4. M-sweeps detection performance of OS(21) along with fixed threshold detectors for fluctuating targets of SWIII model when $N = 24$, and $P_{fa} = 1.0\text{E-}6$.

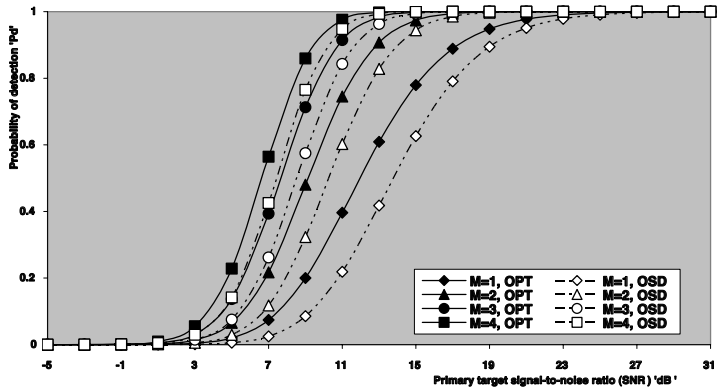

Figure 5. M-sweeps detection performance of OS(21) along with fixed threshold detectors for fluctuating targets of SWIV model when $N = 24$, and $P_{fa} = 1.0\text{E-}6$.

detection performance of the same scheme, for the same parameter values, is included in these families of curves to take an idea about to what extend the noncoherent integration does improve the processor performance. For low values of SNR, the detection performance for SWI is higher than that for SWIII which in turn higher than that for SWII and it attains its lowest value for SWIV. When the SNR becomes stronger, on the other hand, the processor performance is

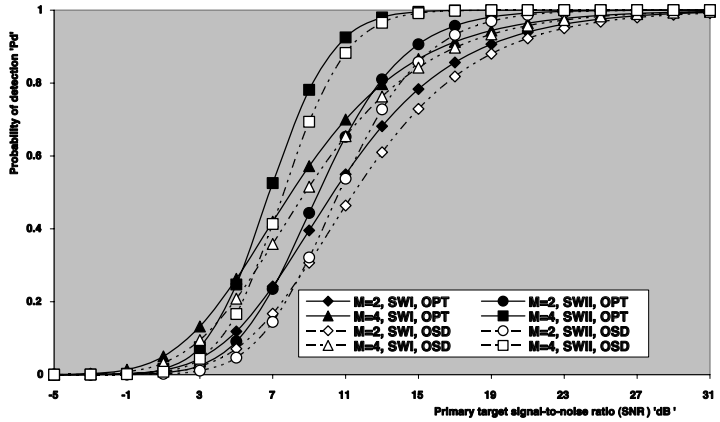

Figure 6. M-sweeps detection performance of OS(21) along with fixed threshold detectors for chi-square fluctuating targets with two-degrees of freedom when $N = 24$, and $P_{fa} = 1.0\text{E-}6$.

reversed which means that it attains its highest value for SWIV which in turn higher than that for SWII and the worst detection curve is for SWI model. In the single sweep case, the detection processor behaves the same behavior taking into account that SWII tends to SWI and SWIV tends to SWIII for the case of monopulse detection. It is important to note that for $M = 2$, the detection performance of the processor under consideration for SWIII model is the same as its behavior against SWII model. In addition, we note that the curves of these families are functions of the number of postdetection integrated sweeps and the detection processor. As predicted, these figures illustrate the superiority of the fixed-threshold scheme over the adaptive-threshold scheme in achieving the homogeneous detection of fluctuating targets under the same parameter values and for the same underling target model. After we took an idea about the detection behavior of the fixed- and adaptive-threshold schemes against each type of Swerling fluctuation models individually, let us now go to compare their behaviors against each family of the same degree of freedom of the chi-square distribution forms. The second category of curves, which includes Figs. 6–7, displays a comparison between the reactions of adaptive- and fixed-threshold procedures to the detection of the four cited target fluctuation models when the radar receiver noncoherently integrates 2 and 4 consecutive sweeps, respectively, in homogeneous environment. The results of these figures confirm our previous conclusion which is associated with the processor performance

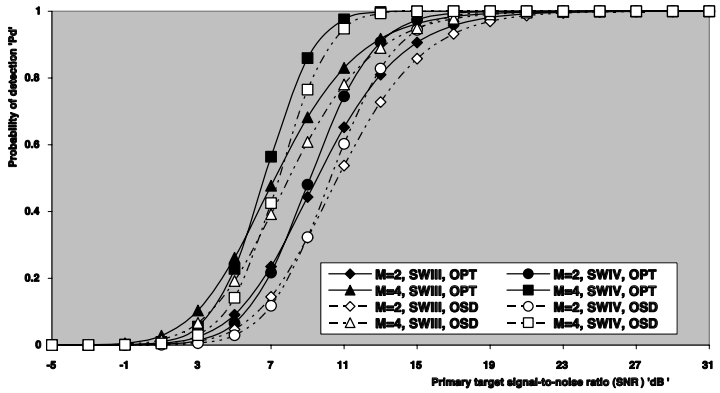

Figure 7. M-sweeps detection performance of OS(21) along with fixed threshold detectors for chi-square fluctuating targets with four-degrees of freedom when $N = 24$, and $P_{fa} = 1.0\text{E-}6$.

against χ^2 fluctuation model with two-degrees of freedom when the signal strength is weak versus the same processor performance under the same fluctuation model of the same degree of freedom when the target strength strong. In other words, the processor reaction against SWI model is higher than its reaction against SWII model for low SNR and this behavior is rapidly changed to its inverse fashion as the SNR increases. For χ^2 model with four-degrees of freedom, the detection scheme behaves the same behavior and this behavior is common either for fixed-threshold or for adaptive-threshold technique. As predicted, these figures demonstrate the superiority of the fixed-threshold scheme over the adaptive-threshold one in achieving the homogeneous detection of fluctuating targets under the same parameter values and for the same underling target model.

Now, let us turn our attention to the multiple-target situations and what happens to the performance of the adaptive-threshold detector when the reference channel, from which the noise power level is estimated, is contaminated with returns from extraneous targets. These effects are illustrated in the third category of curves which includes Figs. 8–10 for the different fluctuation models of Swerling. In obtaining the results of these figures, we assume that there are a three cells amongst the contents of the reference channel which are contaminated with interfering target returns ($r = 3$). It is important to note that this is the maximum allowable value of spurious target returns that may exist amongst the candidates of the reference window before the processor performance becomes degraded [12]. Fig. 8

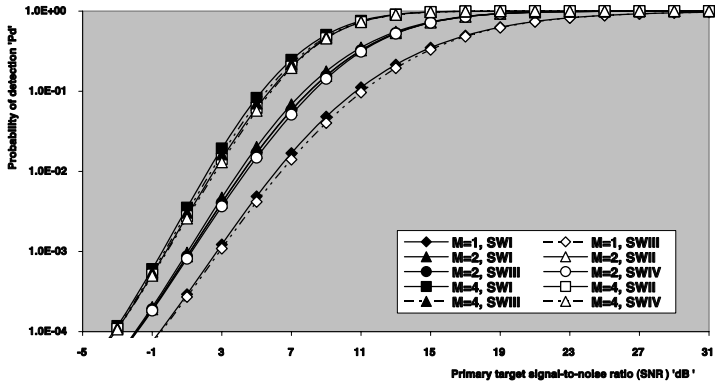

Figure 8. Multitarget M-sweeps detection performance of OSD(21) for Swerling fluctuating targets when the primary target fluctuates according to SWII model, $N = 24$, $P_{fa} = 1.0\text{E-}6$.

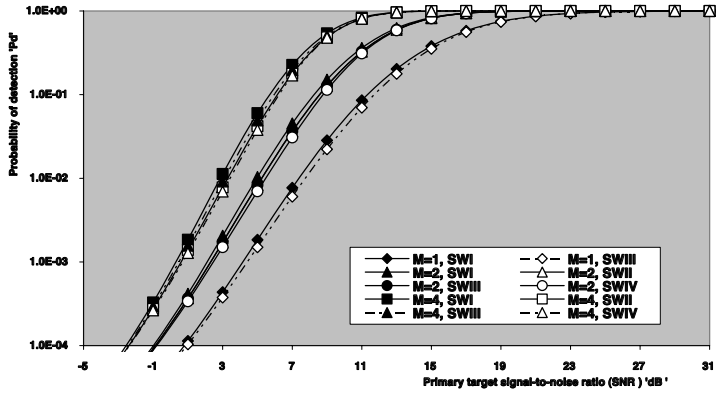

Figure 9. Multitarget M-sweeps detection performance of OSD(21) for Swerling fluctuating targets when the primary target fluctuates according to SWIV model, $N = 24$, $P_{fa} = 1.0\text{E-}6$, and $r = 3$.

depicts the detection performance of OS(21) scheme in multiple-target environments when the primary fluctuates following SWII model and the secondary interfering targets fluctuate obeying all the Swerling fluctuation models taking into account that the radar receiver postdetection integrates M-consecutive pulses. It is to be noted that the interfering target return is of the same strength as the primary target. (INR=SNR). The curves of this family are characterized by the number of integrated pulses as well as the target fluctuation

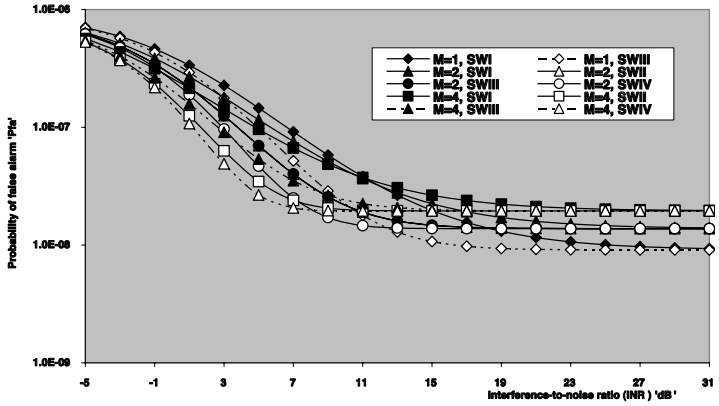

Figure 10. M-sweeps false alarm rate performance of OSD(21) for chi-square fluctuating targets when $N = 24$, and $P_{fa} = 1.0\text{E-}6$, and $r = 3$.

model of the secondary outlying target. From the outlying results of these figures, it is observed that the processor performance attains its maximum behavior when the interfering target fluctuates following SWI model while its worst behavior occurs when the extraneous target fluctuation model becomes of SWIV type. This behavior is common irrespective of the number of integrated pulses or the fluctuation model according to which the secondary interfering target fluctuates. In addition, there is an improvement in the probability of detection as the number of noncoherently integrated pulses increases and this common either in homogeneous or multitarget situation. To show the effect of outlying target returns on the CFAR property of adaptive-threshold detector, Figs. 10 shows the actual false alarm rate performance, as a function of the strength of the level of interference, when the reference cells are contaminated with interfering target returns and the designed level of false alarm is of the order of 10^{-6}. The candidates of this set are labeled in the number of integrated pulses (M) and the fluctuation model of the outlying target. The label ($M = 2$, SWIV) on a specified curve means that it is plotted when the spurious target fluctuates in accordance with SWIV model and for $M = 2$. The results of this figure show that as the interference level increases, the rate of false alarm decreases till a certain value after which it becomes of constant value irrespective of the interference level. The rate of decreasing increases as M increases while the level of interference at which the false alarm rate attains its constant level decreases. In addition, the rate of decreasing for χ^2 distribution with four-degrees of freedom is

higher than that for the same distribution with two-degrees of freedom. Moreover, the steady-state level of false alarm increases as the number of integrated pulses increases. From the CFAR property point of view, the processor performance in the presence of SWI outlying targets is the best one relative to the other fluctuation models of spurious targets. In other words, the rate of decreasing of the false alarm in the case of SWI fluctuation model is slower than that in the case of SWII model which in turn slower than SWIII and SWIV model has the worst behavior of false alarm rate which must be held constant.

Finally, the last category, Figs. 11–15, displays the required SNR, to achieve an operating point of (P_{fa}, P_d) where the designed value of P_{fa} is 10^{-6}, of the procedure under consideration, as a function of the detection probability, when this scheme operates in an ideal as well as in multitarget environments and the radar receiver postdetection integrates 2 and 4 consecutive pulses. For the sake of comparison, the single pulse required SNR is also included in these figures under the same fluctuation model of the primary and the secondary interfering targets. Fig. 11 depicts the required SNR in "dB" of OS(21) scheme when the operating environment is free of any target (homogeneous) except that one under consideration (primary target) which fluctuates following the four fundamental types of Swerling. The curves of this figure are functions of M and fluctuation type. From the displayed results in this figure, we show that the SNR required to achieve a specified P_d increases as P_d increases and the rate of increasing is not linear. In addition, for the same parameter values, the required SNR in the case where the primary target fluctuates following χ^2 distribution with four degrees of freedom is lower than that required when the underlined target fluctuates following χ^2 distribution with two-degrees of freedom. Moreover, the required SNR decreases as the number of noncoherently integrated pulses increases. As expected, the SWIV model requires the minimum SNR to attain the requested values, the SWII comes in the second class, the SWIII model needs higher values of SNR, and SWI case needs the highest values of SNR to arrive to the same levels of detection and false alarm. This behavior is common irrespective of the number of integrated pulses. To give an explicit idea about the variation of the required SNR with the fluctuation model of the target, Figs. 12–13 display this important parameter for the CFAR detector under consideration when the target fluctuates following χ^2 distribution with two and four degrees of freedom, respectively. These figures demonstrate our previous conclusion. Similarly, Figs. 14–15 show the same response when the operating environment contains three outlying targets ($r = 3$) along with the target under consideration in the case where these targets fluctuate following χ^2 distribution with

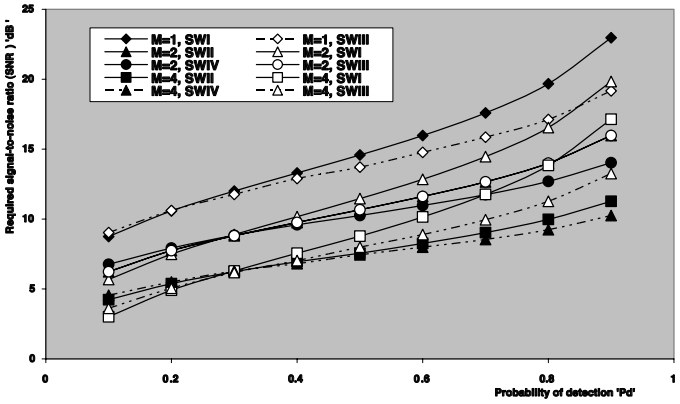

Figure 11. M-sweeps required SNR as a function of the detection probability of OSD(21) for chi-square fluctuating targets when $N = 24$, design $P_{fa} = 1.0\text{E-}6$.

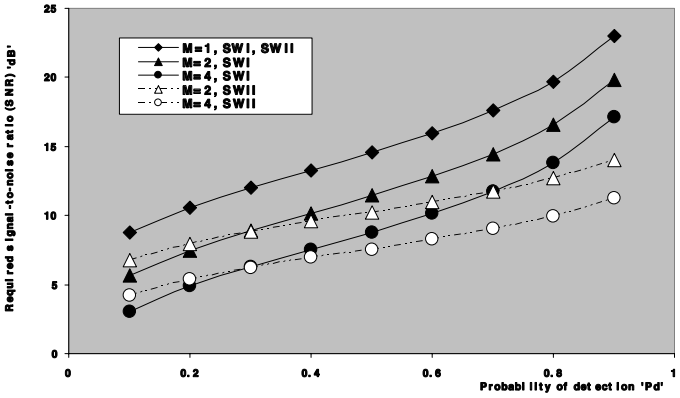

Figure 12. M-sweeps required SNR as a function of the detection probability of OSD(21) processor, in ideal situation, for chi-square fluctuating targets with two-degrees of freedom when $N = 24$, and $P_{fa} = 1.0\text{E-}6$.

two and four degrees of freedom, respectively. The curves of these families are characterized by M, fluctuation model of the primary target, and fluctuation model of the secondary interfering target, respectively. These figures illustrate that the required SNR depends mainly on the fluctuation model of the primary target and then comes the model of the spurious target. It is well known SWII requires lower SNR for higher values of P_d than SWI for any number of integrated

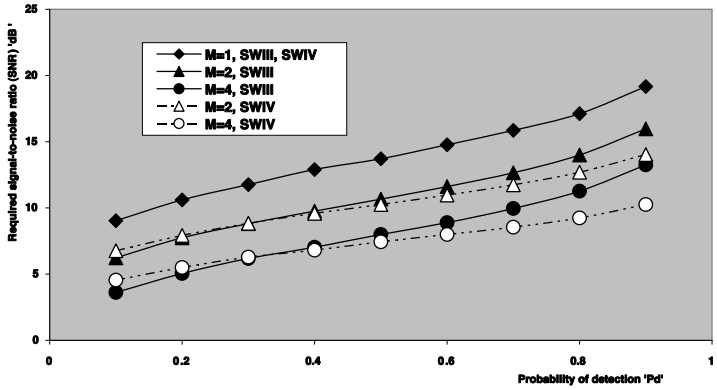

Figure 13. M-sweeps required SNR as a function of the detection probability of OSD(21) processor, in ideal situation, for chi-square fluctuating targets with four-degrees of freedom when $N = 24$, and $P_{fa} = 1.0\text{E-}6$.

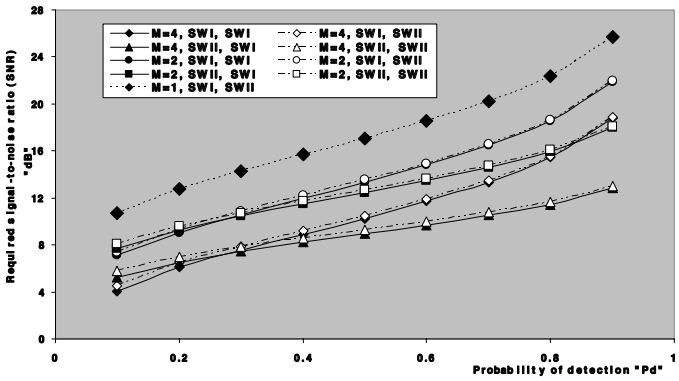

Figure 14. M-sweeps required signal-to-noise ratio of OSD(21) detector to achieve an operating point of (1.0E-6, P_d) for chi-square fluctuating targets with two-degrees of freedom when $N = 24$, and $r = 3$.

pulses. This actually the case of our results when the primary target fluctuation model follows SWII, as Fig. 14 shows. For the same fluctuation model of the primary target, SWI model of the secondary target gives lower SNR than SWII model for the parameter values. This behavior is standard for our chosen parameter values cited here and is independent on the number of integrated pulses. Fig. 15 depicts the same thing for χ^2 distribution with four degrees of freedom and

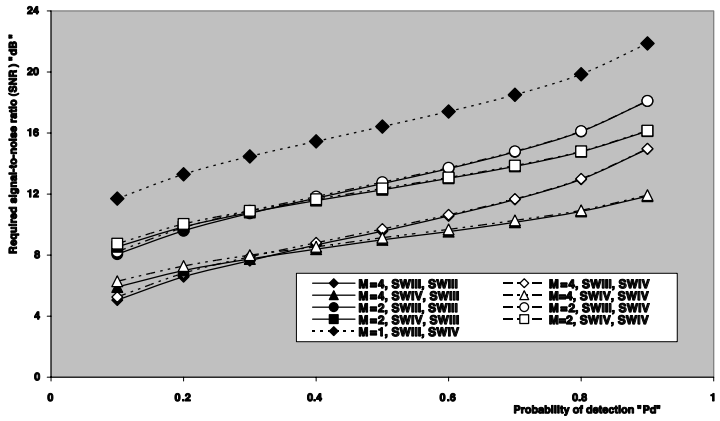

Figure 15. M-sweeps required signal-to-noise ratio of OSD(21) detector to achieve an operating point of (1.0E-6, P_d) for chi-square fluctuating targets with four-degrees of freedom when $N = 24$, and $r = 3$.

gives the same conclusion taking into account that SWIV model acts the same behavior as SWII and SWIII behaves as SWI with lower values of SNR required to achieve a specified operating point.

6. CONCLUSIONS

In this paper, we have given a detailed analysis of the detection performance calculation of the fixed-threshold as well as the adaptive-threshold procedures under the condition that the primary and the secondary outlying targets fluctuate following χ^2 fluctuation model with two and four degrees of freedom. The fluctuation rate may vary from essentially independent return amplitudes from pulse-to-pulse to significant variation only on a scan-to-scan basis. A Swerling fluctuating target is a model which describes the fluctuation in target amplitude caused by changes in target aspect angle, rotation, or vibration of target scattering sources or changes in radar wavelength. This fluctuation model includes the classical models of target echo fluctuation which are known as SWI, SWII, SWIII, and SWIV. The correlation coefficient between the two consecutive echoes in the dwell-time is equal to unity for SWI and SWIII models and is zero for SWII and SWIV models. The adaptive-threshold processor is chosen to be the ordered-statistic (OS) scheme owing to its immunity to interfering targets that may be present amongst the candidates of the reference window from which the noise power level is estimated to construct the

detection threshold after multiplying it with a predetermined constant scale factor. The analysis illustrates the utility of the contour-integral approach in determining the CFAR processor performance in the presence of interferers. The analytical results have been used to develop a complete set of performance curves including detection probability in homogeneous and multiple target situations, the variation of false alarm rate with the strength of interfering targets, and the required SNR to achieve a predetermined operating point of fixed levels for detection and false alarm rates. As expected, lower threshold values and consequently higher detection performance is obtained as the number of postdetection integrated pulses increases. However, as the number of integrated pulses increases, the probability of false alarm becomes more sensitive to the bias level and the period of time taken by the CFAR detector to decide if the target is present or not becomes longer. On the other hand, as the signal correlation increases from zero (SWII and SWIV) to unity (SWI and SWIII), more per pulse SNR is required to achieve a prescribed probability of detection. In addition, the processor performance for fluctuating targets of chi-square model with four degrees of freedom is higher than that for chi-square model with two degrees of freedom, given that the same case of signal correlation is held unchanged. On the other hand, the processor performance for SWIV model is higher than that for SWII model and its behavior against SWIII model is higher than its reaction against SWI model.

REFERENCES

1. Swerling, P., "Probability of detection for fluctuating targets," *IRE Transaction on Information Theory*, Vol. IT-6, 269–308, April 1960.
2. Meyer, D. P. and H. A. Mayer, *Radar Target Detection*, Academic Press, 1973.
3. Skolnik, I. M., *Introduction to Radar Systems*, 2nd edition, McGraw-Hill, 1980.
4. Helstrom, C. W. and J. A. Ritcey, "Evaluating radar detection probabilities by steepest descent integration," *IEEE Transactions on Aerospace and Electronic Systems*, Vol. AES-20, No. 5, 624–633, Sept. 1984.
5. Hou, X. Y., N. Morinaga, and T. Namekawa, "Direct evaluation of radar detection probabilities," *IEEE Transactions on Aerospace and Electronic Systems*, Vol. AES-23, No. 4, 418–423, July 1987.
6. Ritcey, J. A., "Detection analysis of the MX-MLD with

noncoherent integration," *IEEE Transactions on Aerospace and Electronic Systems*, Vol. AES-26, No. 3, 569–576, May 1990.

7. El Mashade, M. B., "M-sweeps detection analysis of cell-averaging CFAR processors in multiple target situations," *IEE Radar, Sonar Navig.*, Vol. 141, No. 2, 103–108, April 1994.
8. Swerling, P., "Radar probability of detection for some additional fluctuating target cases," *IEEE Transactions on Aerospace and Electronic Systems*, Vol. AES-33, 698–709, April 1997.
9. El Mashade, M. B., "Performance analysis of the excision CFAR detection techniques with contaminated reference channels," *Signal Processing "ELSEVIER"*, Vol. 60, 213–234, Aug. 1997.
10. El Mashade, M. B., "Partially correlated sweeps detection analysis of mean-level detector with and without censoring in nonideal background conditions," *AEÜ*, Vol. 53, No. 1, 33–44, Feb. 1999.
11. El Mashade, M. B., "Detection analysis of CA family of adaptive radar schemes processing M-correlated sweeps in homogeneous and multiple-target environments," *Signal Processing "ELSEVIER"*, Vol. 80, 787–801, Aug. 2000.
12. El Mashade, M. B., "Target multiplicity performance analysis of radar CFAR detection techniques for partially correlated chi-square targets," *AEÜ*, Vol. 56, No. 2, 84–98, April 2002.
13. El Mashade, M. B., "M-sweeps exact performance analysis of OS modified versions in nonhomogeneous environments," *IEICE Trans. Commun.*, Vol. E88-B, No. 7, 2918–2927, July 2005.
14. El Mashade, M. B., "Target multiplicity exact performance analysis of ordered-statistic based algorithms for partially correlated chi-square targets," Accepted for publication in *IEE Proc. - Radar, Sonar Navig.*
15. El Mashade, M. B., "CFAR detection of partially correlated chi-square targets in target multiplicity environments," Accepted for publication in *Int. J. Electron. Commun. AEÜ.*
16. El Mashade, M. B., "Performance comparison of a linearly combined ordered-statistic detectors under postdetection integration and nonhomogeneous situations," Accepted for publication in *Chinese Journal of Electronics.*